13th Australasian Fluid Mechanics Conference
Monash University, Melbourne, Australia
13-18 December 1998

TURBULENT TAYLOR–COUETTE FLOW

Murray J. RUDMAN and Hugh M. BLACKBURN
CSIRO Building, Construction and Engineering
Graham Road, Highett, Victoria, AUSTRALIA

ABSTRACT

Results from a numerical study of turbulent Taylor–Couette flow are presented. For the case in which the inner and outer cylinders rotate in opposite senses, the mean flow and Reynolds stress distributions exhibit marked asymmetry about the radial mid-'plane', in contrast to the symmetric distributions found in plane Couette flow. These differences are caused by centrifugal accelerations and mean streamline curvature. The radius of the inner cylinder has a significant influence on the turbulent flow and results are consistent with plane Couette flow being the limit of Taylor–Couette flow as the inner radius becomes infinite.

At both inner and outer cylinders a viscous sublayer is observed that obeys the usual linear relationship, $U^+ = y^+$. A log layer is also predicted near both inner and outer cylinders although it is of limited extent due to the comparatively low Reynolds number of the flows. The law of the wall varies significantly from plane Couette flow, is a strong function of radius ratio and is significantly different for the inner and outer cylinders.

INTRODUCTION

Turbulent channel and Couette flows have been used frequently in the analysis of turbulence models and numerical schemes for Direct Numerical Simulation (DNS) and Large Eddy Simulation (LES). The simple geometry of these flows lends itself to straightforward application of a wide variety of numerical schemes. Additionally, the extensive range of experimental data available (especially for channel flow) allows detailed validation of turbulence models and simulation methods to be undertaken.

Two-equation Reynolds averaged approaches for modelling turbulence, such as the k–ϵ model, perform poorly in swirling and rotating flows, and more sophisticated two-point closures such as Reynolds stress models must be employed to obtain satisfactory results. However full Reynolds stress models are computationally expensive to use and prone to poor convergence. Given the importance of swirling flows in a wide range of industrial and aeronautical applications, simpler models that can empirically model the effect of swirl would have significant advantage, and more effort needs to be focused on the effects of swirl on turbulence. There exists an ideal prototype flow for investigations of the effects of swirl — Taylor–Couette flow.

Depending on the radius ratio and inner and outer cylinder Reynolds numbers, a large range of flow regimes arise. When both cylinders rotate in the same sense, with the inner cylinder rotating more rapidly than the outer cylinder, the canonical flow is a vortex flow, with pairs of counter-rotating 'donut'-shaped vortices existing throughout the vessel for values of the inner Reynolds number beyond a critical value, Re_C. This basic vortex structure exists well into the flow regime that is genuinely turbulent. Transition to turbulence in this case occurs via a gradual process in which additional frequencies slowly appear in the energy spectra with increasing Reynolds number (Brandstater and Swinney 1987).

When the cylinders rotate in opposite directions, the number of possible flow states is smaller and the transition to turbulence occurs more rapidly as the Reynolds number increases. For a fixed outer rotation rate, as the inner rotation rate increases, cylindrical Couette flow develops laminar spiral vortices, rapidly followed by intermittent turbulent 'bursts' that eventually increase in size and merge with each other to form 'spiral turbulence'. Finally, according to Andereck et al. (1986), 'featureless turbulence' results in which no very large scale vortex structures can be visually observed.

In this paper, a DNS technique is used to examine turbulent Taylor–Couette flow in vessels with radius ratios of $\eta = R_I/R_O = 0.875$ and 0.667. For both radius ratios, counter-rotating cylinders are examined at a Reynolds number of 3 000 (based on the velocity difference between cylinders and the gap width). For counter rotating cylinders this choice delivers a flow in the 'featureless turbulence' regime (Andereck et al. 1986).

STABILITY OF SWIRLING FLOWS

When rotation is applied to turbulent Poiseuille flow, the flow on the anti-cyclonic side of the channel is destabilised and flow on the cyclonic side is stabilised.

(The cyclonic side is the side on which the vorticity of the boundary layer has the same sign as the rotation.) In contrast, addition of a forced rotation either stabilises or destabilishes plane Couette flow in the same sense throughout the fluid depending on the sign and magnitude of the additional rotation (Komminaho et al. 1995, Bech et al. 1997). This difference arises because the mean spanwise vorticity in plane Couette flow has the same sign throughout.

Taylor–Couette flow bears some resemblance to plane Couette flow that has been subjected to rotation about a spanwise axis and we may expect some similarities to exist between these two flows. To illustrate the equivalence, compare non-rotating Couette flow to Taylor–Couette flow in which the cylinders rotate in opposite senses. Addition of a cyclonic rotation stabilises Couette flow and changes counter-rotating Taylor–Couette flow toward outer rotating TC flow (see Figure 1a) which is stable, even for very high outer cylinder rotation rates. Addition of anticyclonic rotation destabilises rotating Couette flow and moves counter-rotating Taylor–Couette flow toward inner-rotating TC flow (see Figure 1b) which is unstable for very low rotation rates.

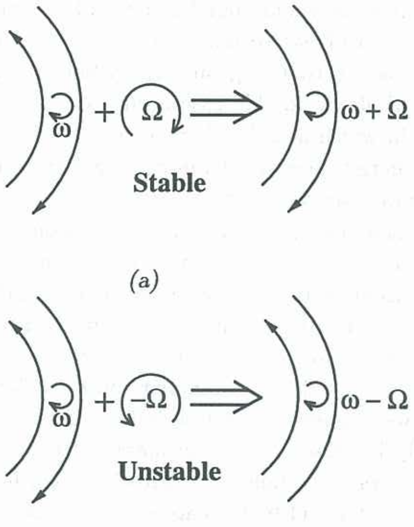

(a)

(b)

Figure 1: Effect of adding rotation to counter rotating Taylor–Couette flow. (a) Cyclonic rotation stabilises, (b) Anticyclonic rotation destabilises.

The criterion for stability of a laminar swirling flow with swirl velocity V is (Chandrasekhar 1981 § 66)

$$\frac{V}{r^2}\frac{\partial(rV)}{\partial r} > 0.$$

This is often written in terms of a Richardson number, or (after Tritton 1992) a Bradshaw number,

$$B = \left(2\frac{V}{r^2}\frac{\partial(rV)}{\partial r}\right) / \left(r\frac{\partial}{\partial r}\left(\frac{V}{r}\right)\right)^2. \quad (1)$$

Equation 1 is equivalent to the criterion for a rotating flow (see Equation 4, Tritton 1992) except that V is replaced by Ωr, where Ω is the angular velocity in the case of forced rotation. In the case where cylinders rotate in opposite senses, B must be negative near the inner cylinder and positive near the outer cylinder, thus destabilising the flow near the inner cylinder and stabilising it near the outer. In this regard, Taylor–Couette flow is fundamentally different to the rotating Couette flows discussed by Komminaho et al. (1995) and Bech and Andersson (1997) in which the axis of rotation passes through the centre of the channel. In that case B has the same sign throughout the flow.

NUMERICAL METHOD

The numerical method is a spectral/spectral-element method in which a 2-D Galerkin spectral element method in the r-z plane is extended into the θ-direction in Fourier space. The method is outlined in Tomboulides et al. (1993). Our implementation runs in parallel using MPI message passing

When choosing a domain size for DNS it is important to ensure that the predicted flow field is not constrained by the domain. The domain sizes chosen here are similar to those of Bech and Andersson which were shown to be adequate. For Couette flow and Taylor–Couette flow with $\eta = 0.875$ the dimensions were $1 \times 2\pi/3 \times 2\pi$ in the wall normal, streamwise and spanwise directions. The discretisation in wall-normal/spanwise planes was 6×20 spectral elements with $8th$ order basis functions and 96 Fourier planes in the streamwise direction. For Taylor–Couette flow with $\eta = 0.667$ the domain size was $1 \times pi \times 2\pi$ with the same spectral element discretisation and 48 Fourier planes. For the Reynolds numbers considered here, placement of nodes corresponds to the first point away from the wall lying at a value of approximately $y^+ = 0.5$.

Two-point velocity fluctuation correlations in the streamwise direction on the centre-plane (not shown) were of order 0.1 at a separation of half the domain length, indicating that an increased domain length may be desirable. There is a small oscillatory component to the correlations in the spanwise direction, suggesting a large scale vortex structure may exist. In the time-mean velocity field there is some evidence of a weak time-mean vortex structure, however its magnitude is only 2% of the difference in swirl velocity between the two cylinders, and continues to decrease as averages are gathered over longer times.

The torque predicted on the inner cylinder (for a case of inner cylinder rotation only at a Reynolds number of 3000) was compared to the torque measurements of Taylor (1936) and the simulation results of Hirschberg (1992) and agreement was within the experimental and numerical scatter reported in those two studies.

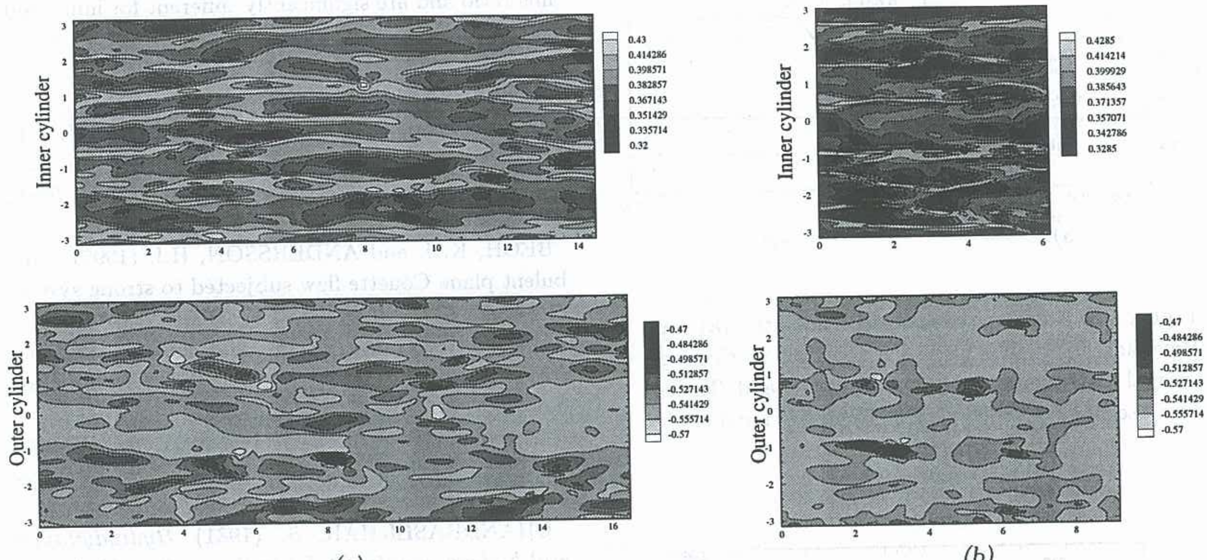

(a) (b)

Figure 2: Streamwise velocity for Taylor–Couette flow at $y^+ = 1.5$: (a) $\eta = 0.875$, and (b) $\eta = 0.667$.

RESULTS

For the case of counter-rotating cylinders, inner and outer Reynolds numbers of $Re_I = 1,286$ and $Re_O = -1,714$ are used. For a radius ratio of $\eta = 0.875$, this corresponds to flow inside the regime labelled 'featureless turbulence' by Andereck (1986).

Contours of instantaneous streamwise velocity on cylindrical surfaces $y^+ = 1.5$ distant from the inner and outer cylinders are shown in Figure 2a for $\eta = 0.875$ and Figure 2b for $\eta = 0.667$. The streak structure on the inner cylinders is clearly visible and the spacing of the structures is approximately the distance between cylinders (this is also seen in the spanwise velocity correlations). The flow structure on the outer cylinders is significantly different to the inner, with fewer and weaker streaks for $\eta = 0.875$ and almost no streaks at all for $\eta = 0.667$. The absence of streaks is indicative of turbulence damping and bears a similarity to Poiseuille flow subjected to rotation.

A plot of B (see Equation 1) versus wall normal position shown in Figure 3. The negative values of B near the inner cylinder and positive values near the outer are consistent with the predicted destabilisation of the flow near the inner cylinder and stabilisation near the outer. For $\eta = 0.667$ the comparatively higher value of B near the outer cylinder (compared to $\eta = 0.875$) is reflected in the damped wall structures seen in Figure 2b.

The mean streamwise velocity profile for Taylor-Couette flow is quite similar to that of plane Couette flow without rotation (Figure 4). However the anti-symmetry of the Couette flow profile no longer applies. Because the torque on the inner and outer cylinders must balance, the effect of reducing η (increasing the curvature of the walls) is to increase the mean wall shear stress at the inner cylinder and decrease it at the outer. The wall shear stress values at inner and outer cylinders bracket the value obtained in plane Couette flow at the same Reynolds number. For $\eta = 0.667$ the wall shear stress is approximately 1.4 times higher than plane Couette flow at the inner cylinder and 0.6 times at the outer. These results suggest that plane Couette flow can be viewed as the limit of counter-rotating Taylor–Couette flow as the radius ratio approaches unity.

The differences in wall shear stress influence the mean streamwise velocity profiles when plotted in wall coordinates (Figure 5). Close to the cylinder walls, the usual linear relationship, $U^+ = y^+$ is obeyed by all profiles although the transition to a log region is delayed on the outer cylinder, especially for high curvature (smaller η) and enhanced on the inner cylinder, again more so high curvature.

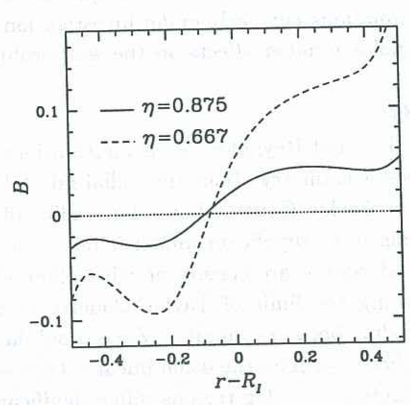

Figure 3: B as a function of wall normal position.

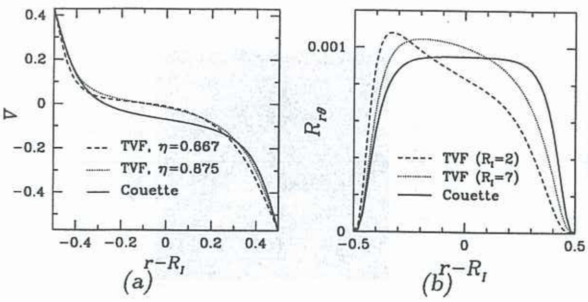

Figure 4: Mean streamwise velocity (a) and Reynolds stress $R_{r\theta}$ (b) as a function of the wall-normal coordinate for plane Couette and Taylor–Couette flows at at equivalent Reynolds numbers.

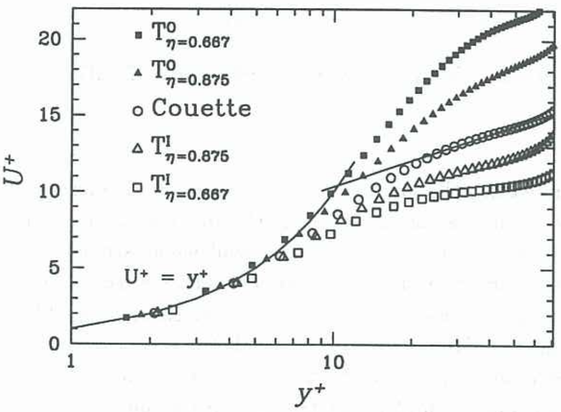

Figure 5: Mean streamwise velocity plotted in wall units. A line with $U^+ = 4.6 + 2.5 \ln y^+$ has been drawn through the log region of Couette flow.

Although the Reynolds number of the simulations is quite low and a broad logarithmic region does not exist in these flows, the results show that the wall profiles are significantly altered, suggesting that law of the wall boundary conditions that are widely used in Reynolds–averaged turbulence models need to be adjusted in flows with significant swirl. Higher Reynolds number simulations currently under investigation will assess Reynolds number effects on the wall profiles.

SUMMARY

The mean flow and Reynolds stress distributions exhibit marked asymmetry about the radial mid-'plane' in Turbulent Taylor–Couette flow. The radius of the inner cylinder has a significant influence on the turbulent flow and results are consistent with plane Couette flow being the limit of Taylor–Couette flow as the inner radius becomes infinite. Viscous sub-layers are are predicted to obey the usual linear relationship at both cylinders. The log regions differ significantly from plane Couette flow, are strong functions of radius ratio and are significantly different for inner and outer cylinders.

REFERENCES

ANDERECK, C.D., LIU, S.S. and SWINNEY, H.L. (1986) 'Flow regimes in a circular Couette system with independently rotating cylinders', *J. Fluid Mech.* **164** 155–183.

BECH, K.H. and ANDERSSON, H.I. (1997) 'Turbulent plane Couette flow subjected to strong system rotation', *J. Fluid Mech.* **347** 289–314.

BRADSHAW, P. (1969) 'The analogy between streamline curvature and buoyancy in turbulent shear flow', *J. Fluid Mech.* **36** 177–191.

BRANDSTATER, A. and SWINNEY, .H.L. (1987) 'Strange attractors in weakly turbulent Couette-Taylor flow', *Phys. Rev. A* **35** 2207–2220.

CHANDRASEKHAR, S. (1981) *Hydrodynamic and hydromagnetic stability* Dover, New York.

HIRSCHBERG, S., (1992), ' Numerical simulation of turbulent Taylor Couette flow', in *Ordered and turbulent patterns in Taylor-Couette flow*, Eds C.D. Andereck and F. Hayot, Plenum Press, New York 149–157.

KOMMINAHO, J., LUNDBLADH, A. and JOHANSSON, A.V., (1996) 'Very large structures in plane turbulent Couette flow', *J. Fluid Mech.* **320** 259–285.

MARCUS, P.S. (1984) 'Simulation of Taylor–Couette flow. Part 2. Numerical results for wavy-vortex flow with one travelling wave', *J. Fluid Mech.* **146** 65-113.

SMITH, G.P. and TOWNSEND, A.A., (1982) 'Turbulent Couette flow between concentric cylinders at large Taylor numbers', *J. Fluid Mech.* **123** 187–217.

TAYLOR, G.I. (1936) 'Fluid friction between rotating cylinders. I–Torque measurements' *Proc. Royal Soc. Lond. A* **157** 546–564.

TOMBOULIDES, A.G., ORSZAG, S.A. and KARNIADAKIS, G.E. (1993) 'Direct and large-eddy simulation of axisymmetric wakes', AIAA Paper No.92-0546, 31st Aerospace Sciences Meeting and Exhibit, January 11–14 Reno NV.